[20]S. L. Altman and C. J. Bradley, Proc. Phys. Soc. (London) 92, 64 (1967); G. S. Fleming and T. L. Loucks, Phys. Rev. 173, 685 (1968).
[21]M. B. Salamon, Phys. Rev. Letters 26, 704 (1971).
[22]H. E. Flotow and D. W. Osborne, Phys. Rev. 160, 467 (1967).
[23]Inasmuch as the spin polarization may be enhanced by conduction-electron–conduction-electron exchange effects [R. E. Watson, in *Hyperfine Interactions*, edited by A. J. Freeman and R. B. Frankel (Academic, New York, 1967), p. 413], the range of β is bounded by $N(E_F) \lesssim N_x(E_F)$, which yields $\beta \lesssim 2.5 \times 10^{-17}$ emu.

PHYSICAL REVIEW B VOLUME 5, NUMBER 3 1 FEBRUARY 1972

Dipolar and Quadrupolar Ordering in $S=\frac{3}{2}$ Ising Systems*

J. Sivardière† and M. Blume
Physics Department, Brookhaven National Laboratory, Upton, New York 11973
(Received 3 August 1971)

We have studied in the molecular-field approximation the statistical-mechanical properties of the Hamiltonian

$$\mathcal{H} = -h\sum_i S_i^z - \sum_{i,j} J_{ij} S_i^z S_j^z - \sum_{i,j} K_{ij} [(S_i^z)^2 - \tfrac{1}{3}S(S+1)]\,[(S_j^z)^2 - \tfrac{1}{3}S(S+1)]$$

for $S=\frac{3}{2}$ ions. We investigate the possibility of ordering in the independent parameters $M=\langle S^z\rangle$ and $Q=\langle (S^z)^2 - \frac{1}{3}S(S+1)\rangle$. The phase diagram is discussed for positive and negative biquadratic interactions as a function of the ratio of bilinear to biquadratic interactions and as a function of the magnetic field h. Successive phase transitions and triple, critical, and tricritical points are found. We also show that the model gives a qualitative understanding of the phase transitions observed in $DyVO_4$.

I. INTRODUCTION

In molecular crystals, the existence of both dipolar and quadrupolar interactions between the molecules may lead to successive orientational transitions, as shown by Krieger and James.[1] Similar behavior is found in magnetic systems, where it is possible to define two different order parameters, the ordinary magnetization $M=\langle S^z\rangle$ and the quadrupolar order parameter $Q=\langle (S^z)^2 - \frac{1}{3}S(S+1)\rangle$. For instance, Blume and Hsieh[2] have considered a Heisenberg Hamiltonian for $S=1$ ions with quadratic and biquadratic exchange interactions and discussed the phase diagram as a function of the ratio of these two types of interactions. $S=1$ Ising models with quadrupolar interactions have been investigated by other workers.[3–7]

In connection with recent experimental results on successive phase transitions in $DyVO_4$,[8–10] we have studied the statistical-mechanical properties of the Ising-like Hamiltonian

$$\mathcal{H} = -h\sum_i S_i^z - \sum_{i,j} J_{ij} S_i^z S_j^z - \sum_{i,j} K_{ij}[(S_i^z)^2 - \tfrac{1}{3}S(S+1)] \times [(S_j^z)^2 - \tfrac{1}{3}S(S+1)] \quad (1)$$

for N ($S=\frac{3}{2}$) ions on a lattice. This Hamiltonian is not directly applicable to $DyVO_4$ because the energy-level scheme is not that of an effective spin $\frac{3}{2}$ nor are the interactions in that substance strictly Ising-like. We expect the *qualitative* picture, however, to be correct. The interactions J_{ij} and K_{ij} can arise from a number of different physical processes. We refer to them as the "dipolar" and "quadrupolar" interactions, respectively, but we do not necessarily imply that they arise from magnetic dipole-dipole or electric quadrupole-quadrupole interactions. The names are convenient because they suggest that the interactions can produce dipolar or quadrupolar order, as defined above. The quadrupolar interaction K_{ij} could arise, for example, from biquadratic exchange[11,12] due to the presence of the orbital moment, or from bilinear exchange projected into the low-lying levels of a multiplet, so that in a spin Hamiltonian the form of the interaction becomes complex.[11,12] Alternately, it could result from phonon exchange between ions, in which case one might refer to a "cooperative Jahn-Teller effect." The thermodynamic properties of the system will, however, be independent of the origin of the exchange interaction and we therefore consider these properties here. Separate experiments are required in order to determine the physical origin of the parameters J_{ij} and K_{ij}. A study of the elementary excitations (e.g., phonons, librons, and magnons) and their interactions can distinguish between the various possible mechanisms and can determine whether lattice distortions, which accompany the phase transitions, are essential to or incidental to their occurrence.

We first derive self-consistent equations for the order parameters M and Q in the molecular-field

approximation. For spin $\frac{3}{2}$ it is in general also necessary to consider "octupolar" ordering with a parameter which depends on $\langle (S^z)^3 \rangle$. We do not do so here because the Hamiltonian (1) does not contain "cubic" exchange of the form $(S_i^z)^3(S_j^z)^3$, so the octupole-order parameter is not driven directly by the interactions.

In Sec. II, we discuss the phase diagram for fixed positive quadrupolar interactions and varying dipolar interactions in zero external field. We find that for a range of the parameters J_{ij} and K_{ij}, two separate second-order phase transitions occur. At a higher temperature, there is a transition to a state of nonzero quadrupolar order, but zero magnetic order. At a lower temperature, a second transition occurs to a state of nonzero magnetic order. As the parameters change, the two transitions eventually are found to occur at the same temperature and in another regime they become first-order transitions. We also investigate the influence of a magnetic field on the phase diagram, and the case of negative quadrupolar interactions. Finally, we discuss the suggestive similarities between the behavior of our model and the observed properties of $DyVO_4$.

II. MOLECULAR-FIELD APPROXIMATION

We first restrict ourselves to positive dipolar and quadrupolar interactions and introduce their Fourier transforms

$$J \equiv J(0) = \sum_j J_{ij} \tag{2a}$$

and

$$K \equiv K(0) = \sum_j K_{ij} \ . \tag{2b}$$

Let H and σ be the molecular fields associated with the order parameters $M = \langle S^z \rangle$ and $Q = \langle (S^z)^2 - \frac{5}{4} \rangle$. In the molecular-field approximation, the one-ion Hamiltonian $\mathcal{H}_0$ is

$$\mathcal{H}_0 = -(H+h)\sum_i S_i^z - \sigma \sum_i [(S_i^z)^2 - \tfrac{5}{4}] \ . \tag{3}$$

The corresponding partition function is $Z_0^N = \mathrm{tr}\, e^{-\beta \mathcal{H}_0}$, where

$$Z_0 = 2e^{\beta\sigma} \cosh \tfrac{3}{2}\beta (H+h) + 2e^{-\beta\sigma} \cosh \tfrac{1}{2}\beta (H+h) \tag{4}$$

and $\beta = 1/kT$. In order to derive equations for H and σ, we use the variation principle for the free energy[7,13] F,

$$F \leq \phi = F_0 + \langle V \rangle_0 \ , \tag{5}$$

where

$$\mathcal{H} = \mathcal{H}_0 + V \ , \tag{6}$$

$$F_0 = -\frac{N}{\beta} \ln Z_0 \ , \tag{7}$$

$$\langle V \rangle_0 = \mathrm{tr} \rho_0 V \ , \tag{8}$$

$$\rho_0 = \frac{e^{-\beta \mathcal{H}_0}}{\mathrm{tr}\, e^{-\beta \mathcal{H}_0}} \ . \tag{9}$$

We find immediately

$$\langle V \rangle_0 = -NJ \langle S^z \rangle_0^2 - NK \langle (S^z)^2 - \tfrac{5}{4} \rangle_0^2 + NH \langle S^z \rangle_0 + N\sigma \langle (S^z)^2 - \tfrac{5}{4} \rangle_0 \ , \tag{10}$$

with

$$\langle S^z \rangle_0 = \frac{1}{Z_0} [3e^{\beta\sigma} \sinh \tfrac{3}{2}\beta (H+h) + e^{-\beta\sigma} \sinh \tfrac{1}{2}\beta (H+h)] = \frac{A}{Z_0} \ , \tag{11}$$

$$\langle (S^z)^2 - \tfrac{5}{4} \rangle_0 = \frac{1}{Z_0} [2e^{\beta\sigma} \cosh \tfrac{3}{2}\beta (H+h) - 2e^{-\beta\sigma} \cosh \tfrac{1}{2}\beta (H+h)] = \frac{B}{Z_0} \ . \tag{12}$$

We get then the following expression for ϕ/N:

$$\frac{\phi}{N} = -\frac{1}{\beta} \ln Z_0 + H\frac{A}{Z_0} + \sigma \frac{B}{Z_0} - J\left(\frac{A}{Z_0}\right)^2 - \sigma \left(\frac{B}{Z_0}\right)^2 \ . \tag{13}$$

H and σ are now determined from the conditions

$$\frac{\partial \phi/N}{\partial H} = \left(H - 2J\frac{A}{Z_0}\right)\left(\frac{A}{Z_0}\right)_H' + \left(\sigma - 2K\frac{B}{Z_0}\right)\left(\frac{B}{Z_0}\right)_H' = 0 \ , \tag{14}$$

$$\frac{\partial \phi/N}{\partial \sigma} = \left(H - 2J\frac{A}{Z_0}\right)\left(\frac{A}{Z_0}\right)_\sigma' + \left(\sigma - 2K\frac{B}{Z_0}\right)\left(\frac{B}{Z_0}\right)_\sigma' = 0 \ , \tag{15}$$

which are satisfied if, and only if,

$$H = 2JA/Z_0 \equiv 2JM \ , \tag{16}$$

$$\sigma = 2KB/Z_0 \equiv 2KQ \ . \tag{17}$$

Finally, M and Q are determined from the following self-consistent equations:

$$M = \frac{3e^{2\beta KQ} \sinh(3\beta JM + \frac{3}{2}\beta h) + e^{-2\beta KQ} \sinh(\beta JM + \frac{1}{2}\beta h)}{2e^{2\beta KQ} \cosh(3\beta JM + \frac{3}{2}\beta h) + 2e^{-2\beta KQ} \cosh(\beta JM + \frac{1}{2}\beta h)} \ , \tag{18}$$

$$Q = \frac{2e^{2\beta KQ} \cosh(3\beta JM + \frac{3}{2}\beta h) - 2e^{-2\beta KQ} \cosh(\beta JM + \frac{1}{2}\beta h)}{2e^{2\beta KQ} \cosh(3\beta JM + \frac{3}{2}\beta h) + 2e^{-2\beta KQ} \cosh(\beta JM + \frac{1}{2}\beta h)} \ , \tag{19}$$

and the free energy is given by

$$\frac{F}{N} = -\frac{1}{\beta} \ln Z_0 + JM^2 + KQ^2 \ . \tag{20}$$

III. PHASE DIAGRAM FOR $J, K > 0$ AND $h = 0$

Before discussing the general situation, let us consider three particular cases [Figs. 1(a)–1(c)]:

(a) $J = 0$; Eqs. (18) and (19) give

$$M = 0 \ , \quad Q = \tanh 2\beta KQ \ . \tag{21}$$

There is no dipolar ordering. Quadrupolar order-

ing ($Q \neq 0$) appears below T_Q ($kT_Q = 2K$), the transition is second order (as for a dipolar ordering in a spin-$\frac{1}{2}$ Ising model), and just below T_Q, $Q \sim (T_Q - T)^{1/2}$. The molecular field σ splits the $S = \frac{3}{2}$ quadruplet into two doublets: $S^z = \pm\frac{3}{2}$ (the ground state), and $S_z = \pm\frac{1}{2}$. We note here that for $J = 0$, we can make rigorous statements about the system which go beyond the mean-field approximation. This is because the system in this case is equivalent to a spin-$\frac{1}{2}$ Ising model. The exact partition function Z is given by

$$Z = \sum_{\{S_i^z\}} \exp\{\beta \sum_{i,j} K_{ij}[(S_i^z)^2 - \tfrac{5}{4}][(S_j^z)^2 - \tfrac{5}{4}]\} ,$$

where each S_i^z takes on the values $\pm\frac{1}{2}$ and $\pm\frac{3}{2}$. Defining $\sigma_i = (S_i^z)^2 - \frac{5}{4}$, we note that $\sigma_i = +1$ when $S_i^z = \pm\frac{3}{2}$ and $\sigma_i = -1$ when $S_i^z = \pm\frac{1}{2}$. Hence,

$$Z = 2^N \sum_{\{\sigma_i\}} \exp(\beta \sum_{i,j} K_{ij}\sigma_i\sigma_j) ,$$

where the factor of 2^N accounts for the two possible values of S_i^z for each σ_i. This is just the partition function for a spin-$\frac{1}{2}$ Ising model, for which the phase transition is second order.

(b) $K = 0$; Eq. (18) gives

$$M = \frac{3\sinh 3\beta JM + \sinh \beta JM}{2\cosh 3\beta JM + 2\cosh \beta JM} \equiv B_{3/2}(\beta JM) . \quad (22)$$

Dipolar ordering appears below $T_{MQ}[kT_{MQ} = \frac{5}{2}J = \frac{2}{3}JS(S+1)]$; the transition is second order and the the $S = \frac{3}{2}$ quadruplet is split into four singlets by the molecular field H. Because of kinematical coupling, $M \neq 0$ implies $Q \neq 0$ (although $K = 0$) as given by Eq. (19) and near T_{MQ}, $M \sim (T_{MQ} - T)^{1/2}$ and $Q \sim M^2 \sim T_{MQ} - T$.

(c) $J \ll K$; since the dipolar interactions are almost negligible, we expect that the quadrupolar transition at T_Q, $kT_Q = 2K$ will be unchanged. Near 0 °K, because $J \neq 0$, dipolar ordering is now possible and M is given by Eq. (18) where $Q \simeq 1$ and $2\beta KQ \sim \infty$: $M = \frac{3}{2}\tanh 3\beta JM$. The transition appears at T_M ($kT_M = \frac{9}{2}J$) and is second order. It involves only the ground-state doublet $S^z = \pm\frac{3}{2}$ (effective spin $\frac{1}{2}$) but the moment is $\frac{3}{2}$ so that $kT_M = 2J(\frac{3}{2})^2 = \frac{9}{2}J$. In this case, we find two well-separated phase transitions as shown in Fig. 1(c).

We now investigate the phase diagram for arbitrary values of J/K. Eliminating $e^{2\beta KQ}$ between (18) and (19), where we put $h = 0$, we get

$$Q = \frac{2M\cosh\beta JM(4\cosh^2\beta JM - 3) - 8\sinh\beta JM\cosh^2\beta JM + 3\sinh\beta JM}{4\sinh\beta JM\cosh^2\beta JM} . \quad (23)$$

Using (23), it is possible to determine the lines in the J, T plane along which second-order phase transitions may appear. We write $\beta JM = x$. For $x \ll 1$,

$$Q = Q_0 + Rx^2 + Sx^4 , \quad (24)$$

where Q_0, R, and S are some functions of J and T. In particular,

$$Q_0 = 1/2\beta J - \tfrac{5}{4} , \quad (25)$$

so that if $M \to 0$ for $T \to T_0$, $Q \to Q_0$: The continuous dipolar transition is also a continuous quadrupolar transition if $T_0 = T_{MQ} = \frac{5}{2}J$ (and $Q \sim M^2$ just below T_{MQ}); there will be a continuous transition from a dipolar to a quadrupolar state at T_M if $Q_0(T_M) \equiv \tanh(2\beta_M K Q_0)$, so that we must have

$$\frac{kT_M}{2J} - \frac{5}{4} = \tanh\left(\frac{K}{J} - \frac{5K}{2kT_M}\right) . \quad (26)$$

Otherwise the transition is first order. Equation (26) may be solved numerically or graphically. One finds always $T_M < 2K$. For very low temperatures (26) gives the solutions $kT_M = \frac{9}{2}J$ and $kT_M = \frac{1}{2}J$ (only in the first case, one has $Q_0 > 0$).

Let us suppose now that a purely quadrupolar transition is possible at T_Q. From (23) with $M = 0$, we get (as when $J = 0$)

$$Q = \tanh 2\beta KQ ,$$

so that $kT_Q = 2K$ and the transition is always second

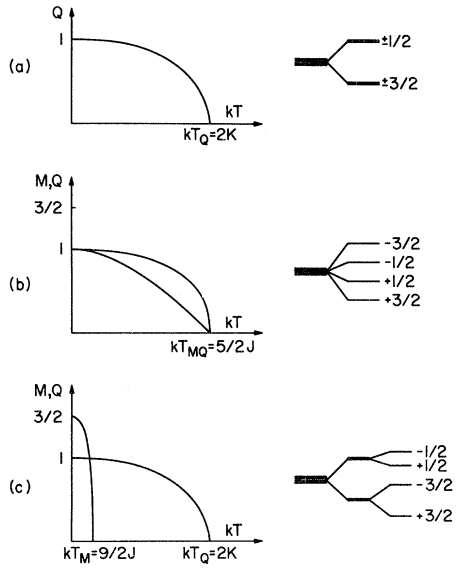

FIG. 1. Thermal variation of the order parameters M and Q and splitting of the quadruplet $S = \frac{3}{2}$ in three particular cases: (a) $K > 0$, $J = 0$; (b) $J > 0$, $K = 0$; and (c) $K \gg J > 0$.

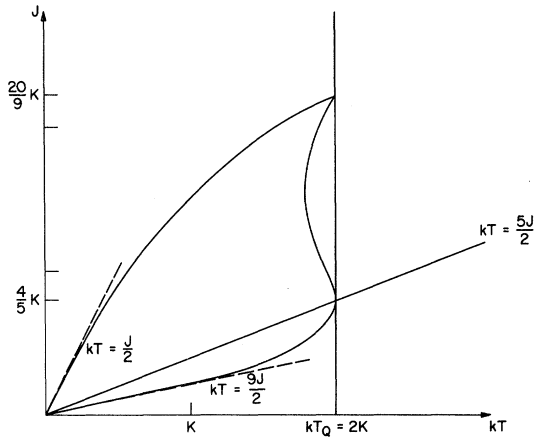

FIG. 2. Possible second-order phase transitions in the J-T plane according to Eq. (23).

order. Finally, Fig. 2 shows the lines in the J, T plane along which second-order phase transitions may appear. The results agree with the above discussion of the three particular cases, $J=0$, $K=0$, and $K \gg J$.

To see which parts of these lines correspond to real second-order phase transitions, we perform a Landau development[14] of the free energy F along these lines, using Eqs. (20) and (24). We write then

$$F = F_0 + A(T, Q_0)M^2 + B(T, Q_0)M^4 + \cdots \qquad (27)$$

(no M^3 term appears in the development). Q_0 is the value of Q at the transition and is given by $Q_0 = \tanh 2\beta K Q_0$. In particular,

$$A(T, Q_0) = 1 + 2R\beta^2 KJ(1+Q_0) - \beta J \frac{1 + e^{4\beta K Q_0}(9 + 8R\beta K)}{2(1+e^{4\beta K Q_0})} . \qquad (28)$$

The transition temperature is given by $A(T, Q_0)=0$, and the transition is second order as long as $B(T, Q_0) > 0$. If $Q_0 = 0$, we find $kT = \frac{5}{2}J$; if $Q_0 \simeq 1$, $kT = \frac{9}{2}J$. If $Q_0 = 0$, $B(T, Q_0)$ is positive for $J > 1.80$; if $Q_0 \neq 0$, $B(T, Q_0)$ is positive for $J < 0.46$.

Finally, the self-consistent equations (18) and (19) have been solved numerically by substituting (23) into (18), and we compared the free energy of three solutions $M = Q = 0$; $M = 0$, $Q = \tanh 2\beta K Q$; $M \neq 0$, $Q \neq 0$. The phase diagram is shown in Fig. 3. Summarizing, we have found: (a) For $J > 1.80$, a single second-order transition to a state where M and $Q \neq 0$, driven mainly by the dipolar interactions. (b) For $1.80 > J > 0.65$, a single first-order transition to a state where M and $Q \neq 0$ (the appearance of a magnetic transition is well known in systems like MnAs[15] where biquadratic exchange may be important). (c) For $0.65 > J > 0.46$, two separate phase transitions; the quadrupolar one is second order, the dipolar one first order. (d) for $0.46 > J > 0$, two separate second-order phase transitions. As we shall see, a similar situation appears in $DyVO_4$. Figure 4 shows the thermal variation of M and Q for the four situations.

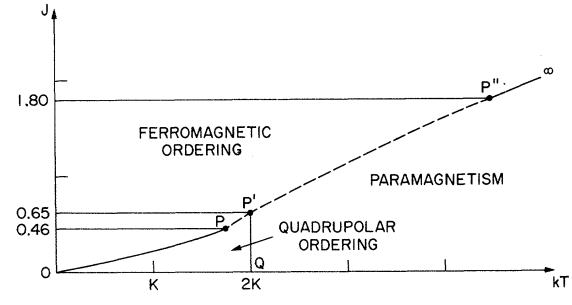

FIG. 3. Phase diagram for $h=0$, J and $K>0$. Dashed lines indicate first-order transitions.

IV. INFLUENCE OF MAGNETIC FIELD

We first suppose that $J=0$ and study the influence of a magnetic field h on the transition at T_Q. Even at high temperature, $M \neq 0$ and, because of the kinematical coupling, $Q \neq 0$ so that the transition is suppressed by h [Fig. 5(a)]. (We have checked that the transition never becomes first order.) As shown in Fig. 5(b), the magnetization presents a bump near $kT = 2K$ when h is small.

We now come back to the general situation.

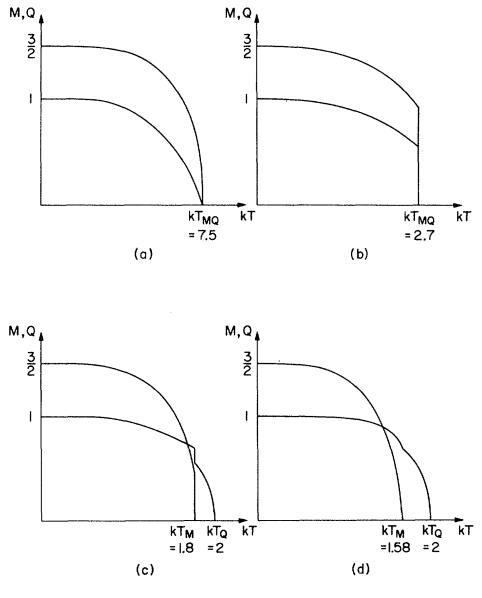

FIG. 4. Thermal variation of M and Q: (a) a single second-order transition ($J=3K$); (b) a single first-order transition ($J=K$); (c) a second-order quadrupolar transition and a first-order dipolar transition ($J=0.5K$); and (d) two second-order transitions ($J=0.4K$).

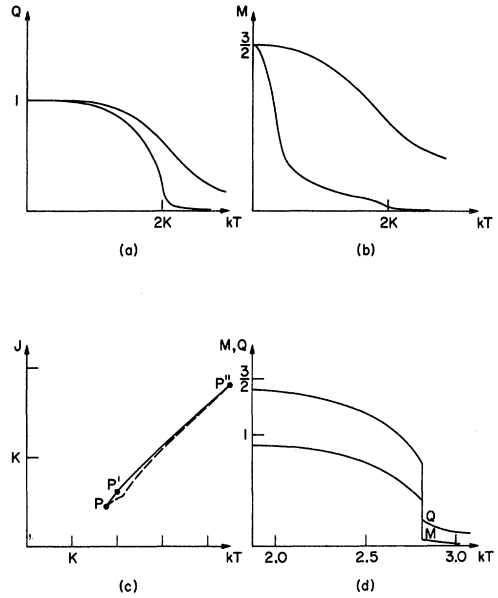

FIG. 5. Influence of h on the phase diagram: (a) and (b) $J=0$; $hS=0.1K$ and $1.0K$; (c) line of critical points (dashed line); and (d) thermal variation of M and Q for $h<h_c$ ($Sh=0.05$; $J=K$).

When h is applied, the second-order lines QP' (quadrupolar transition), OP, and $P''\infty$ (dipolar ferromagnetic transition) disappear, i.e., paramagnetic and quadrupolar regions disappear, so that the system is always ferromagnetic. The first-order transitions along PP'' appear at higher temperatures [Figs. 5(c) and 5(d)] and disappear when h is very large: the surface describing the first-order transitions is limited by a line of critical points, P and P'' are tricritical points.[16] The character of P' could be made precise if the magnetic field were replaced by a crystalline field.

Let us comment briefly on the case where $K>0$ and $J<0$. The dipolar interactions favor an antiferromagnetic ordering, so that we have to divide the lattice into two sublattices A and B and introduce four order parameters Q_A, Q_B, M_A, and M_B. Self-consistent equations for these parameters may be obtained as in Sec. II and, as long as $h=0$, we get

$$Q_A = Q_B \quad \text{and} \quad M_A = -M_B \ ,$$

so that the phase diagrams for $J>0$ and $J<0$ are identical (we have not studied the influence of h). In the same manner when $K<0$ and $h=0$ the phase diagram for $J>0$ and $J<0$ are identical.

V. PHASE DIAGRAM WHEN $K<0$

We introduce two sublattices A and B ($2N$ atoms on the lattice), and the molecular fields σ_A, σ_B, H_A, and H_B. The one-ion Hamiltonian is

$$\mathcal{H}_0 = -N(H_A+h)\sum_{i_A} S^z_{i_A} - N(H_B+h)\sum_{j_B} S^z_{j_B} - N\sigma_A\sum_{i_A}[(S^z_{i_A})^2-\tfrac{5}{4}] - N\sigma_B\sum_{j_B}[(S^z_{j_B})^2-\tfrac{5}{4}] \ . \tag{29}$$

The partition function for A and B ions is

$$Z_A = 2e^{\beta\sigma_A}\cosh\tfrac{3}{2}\beta(H_A+h) + 2e^{-\beta\sigma_A}\cosh\tfrac{1}{2}\beta(H_A+h) \tag{30}$$

and a similar expression for Z_B. $Z_A^N Z_B^N$ is the partition function of the system and

$$\frac{F_0}{N} = -\frac{1}{\beta}\ln Z_A - \frac{1}{\beta}\ln Z_B \ .$$

Consequently,

$$\langle S^z_A\rangle = \frac{1}{Z_A}[3e^{\beta\sigma_A}\sinh\tfrac{3}{2}\beta(H_A+h) + e^{-\beta\sigma_A}\sinh\tfrac{1}{2}\beta(H_A+h)] \ , \tag{31}$$

$$\langle (S^z_A)^2-\tfrac{5}{4}\rangle = \frac{1}{Z_A}[2e^{\beta\sigma_A}\cosh\tfrac{3}{2}\beta(H_A+h) - 2e^{-\beta\sigma_A}\cosh\tfrac{1}{2}\beta(H_A+h)] \ , \tag{32}$$

and similar expressions for $\langle S^z_B\rangle$ and $\langle (S^z_B)^2-\frac{5}{4}\rangle$. We note $\langle S^z_A\rangle = m_A/Z_A$ and $\langle Q^z_A\rangle = q_A/Z_A$, so that

$$\frac{\phi}{N} = -\frac{1}{\beta}\ln Z_A - \frac{1}{\beta}\ln Z_B + H_A\frac{m_A}{Z_A} + H_B\frac{m_B}{Z_B} + \sigma_A\frac{q_A}{Z_A} + \sigma_B\frac{q_B}{Z_B} - J\frac{m_A m_B}{Z_A Z_B} - K\frac{q_A q_B}{Z_A Z_B} \ . \tag{33}$$

The conditions

$$\frac{\partial\phi}{\partial H_A} = \frac{\partial\phi}{\partial H_B} = \frac{\partial\phi}{\partial\sigma_A} = \frac{\partial\phi}{\partial\sigma_B} = 0$$

give

$$\begin{aligned} H_A &= 2J\frac{m_B}{Z_B} = 2JM_B \ , \\ H_B &= 2J\frac{m_A}{Z_A} = 2JM_A \ , \\ \sigma_A &= 2K\frac{q_B}{Z_B} = 2KQ_B \ , \\ \sigma_B &= 2K\frac{q_A}{Z_A} = 2KQ_A \ . \end{aligned} \tag{34}$$

Finally, we obtain four self-consistent equations

$$M_A = \frac{3e^{2\beta KQ_B}\sinh(3\beta JM_B+\frac{3}{2}\beta h) + e^{-2\beta KQ_B}\sinh(\beta JM_B+\frac{1}{2}\beta h)}{2e^{2\beta KQ_B}\cosh(3\beta JM_B+\frac{3}{2}\beta h) + 2e^{-2\beta KQ_B}\cosh(\beta JM_B+\frac{1}{2}\beta h)} \ , \tag{35}$$

$$Q_A = \frac{2e^{2\beta KQ_B}\cosh(3\beta JM_B+\frac{3}{2}\beta h) - 2e^{-2\beta KQ_B}\cosh(\beta JM_B+\frac{1}{2}\beta h)}{2e^{2\beta KQ_B}\cosh(3\beta JM_B+\frac{3}{2}\beta h) + 2e^{-2\beta KQ_B}\cosh(\beta JM_B+\frac{1}{2}\beta h)} \ , \tag{36}$$

$$M_B = \frac{3e^{2\beta K Q_A}\sinh(3\beta J M_A + \frac{3}{2}\beta h) + e^{-2\beta K Q_A}\sinh(\beta J M_A + \frac{1}{2}\beta h)}{2e^{2\beta K Q_A}\cosh(3\beta J M_A + \frac{3}{2}\beta h) + 2e^{-2\beta K Q_A}\cosh(\beta J M_A + \frac{1}{2}\beta h)} , \tag{37}$$

$$Q_B = \frac{2e^{2\beta K Q_A}\cosh(3\beta J M_A + \frac{3}{2}\beta h) - 2e^{-2\beta K Q_A}\cosh(\beta J M_A + \frac{1}{2}\beta h)}{2e^{2\beta K Q_A}\cosh(3\beta J M_A + \frac{3}{2}\beta h) + 2e^{-2\beta K Q_A}\cosh(\beta J M_A + \frac{1}{2}\beta h)} , \tag{38}$$

and the free energy F/N is given by

$$\frac{F}{N} = -\frac{1}{\beta}\ln Z_A - \frac{1}{\beta}\ln Z_B + J M_A M_B + K Q_A Q_B .$$

We first discuss some particular cases (Fig. 6) for $h = 0$.

(a) $J = 0$. Equations (35)–(38) give

$$M_A = M_B = 0 , \qquad Q_A = -Q_B = \tanh 2\beta |K| Q_A . \tag{39}$$

There is no dipolar ordering; "antiquadrupolar" ordering appears at $kT_Q = 2|K|$ and the transition is second order.

(b) $J > 0$, $K = 0$. Dipolar ordering (ferromagnetic state) appears at $T_{MQ} = \frac{5}{2}J$ (see Sec. III).

(c) $J \ll |K|$. Well below T_Q, the dipolar forces impose a dipolar ordering. From (35) to (38) with $Q_A = -Q_B = 1$ we get

$$M_A = \tfrac{3}{2}\tanh 3\beta J M_B ,$$

$$M_B = \tfrac{1}{2}\tanh \beta J M_A .$$

When $T \to 0$, $M_A = \frac{3}{2}$ and $M_B = \frac{1}{2}$ so that we have now a *ferri*magnetic ordering; the transition is second order; it appears at $kT_M = \frac{3}{2}J$ $(= 2J \times \frac{3}{2} \times \frac{1}{2})$.

In order to solve numerically Eqs. (35)–(38), we eliminate $e^{2\beta K}Q_B$ between (35) and (36) and $e^{2\beta K}Q_A$ between (37) and (38), from which $Q_A = f(M_A, M_B)$ and $Q_B = g(M_A, M_B)$. We then substitute into (35) and (37) so that we are left with two equations.

The phase diagram is shown in Fig. 7, which is divided into several regions:

(a) $J > 1.53$. A single second-order phase transition appears to a state where $M_A = M_B \neq 0$, $Q_A = Q_B \neq 0$; $kT_{MQ} = \frac{5}{2}J$.

(b) $1.53 > J > 0.81$. A second transition appears to a state where $M_A \neq M_B$, $Q_A \neq Q_B$; it is second order (it corresponds to a lowering of symmetry since two sublattices appear).

(c) $0.80 > J > 0.30$. Two separate phase transitions: the antiquadrupolar one ($kT_Q = 2|K|$) is second order, the dipolar one is first order.

(d) $0.30 > J > 0$. Two separate second-order phase transitions. Finally, for $J < \frac{4}{3}|K|$, the ground state is ferromagnetic, while for $J < \frac{4}{3}|K|$ it is ferrimagnetic. For $0.81 > J > 0.80$, there are four transitions: two second-order transitions to a ferromagnetic state then a ferrimagnetic state, and two first-order transitions limiting the existence of an intermediate purely antiquadrupolar state. Thermal variations of the order parameters are shown in Fig. 8.

Let us take $J = 0$ and study the influence of a magnetic field on the antiquadrupolar transition. At high temperatures, the system is ferromagnetic; below T_0, it becomes ferrimagnetic [Fig. 9(a)]. The transition temperature is first slightly increased by h, then decreased, and the transition disappears for $h > h_c$ [Fig. 9(b)]. When $J \neq 0$, as shown in Fig. 10, a surface in the $J - h - T$ space separates a ferromagnetic state from a ferrimagnetic state, since a purely antiquadrupolar state is no longer found. Consequently, the second-order lines OP and $P'\infty$ disappear; the first-order transition between two ferrimagnetic states appears at a higher temperature and disappears (line of critical points) so that P and P' may be considered as tricritical points. The surface Σ intersects the three coordinate planes along the lines CQ, QP' and $P'P''$, $P''C$. Finally, at $T = 0\,^\circ\mathrm{K}$, the straight line $h + 3J = 4K$ separates a ferrimagnetic from a ferromagnetic ground state.

VI. APPLICATION TO $DyVO_4$

Two phase transitions are observed in $DyVO_4$: a crystallographic transition at 14 °K, which has been considered as a Jahn-Teller transition, and a second one at 3 °K, which is an antiferromagnetic transition.[17] Both of them are second order, as shown by specific-heat measurements[9] and the thermal variation of the crystal distortion b/a.[10]

Optical studies[18] show that only a ground-state quadruplet (effective spin $S' = \frac{3}{2}$) is involved in the two transitions: This quadruplet is split into two doublets at 14 °K, and then at 3 °K into four singlets,

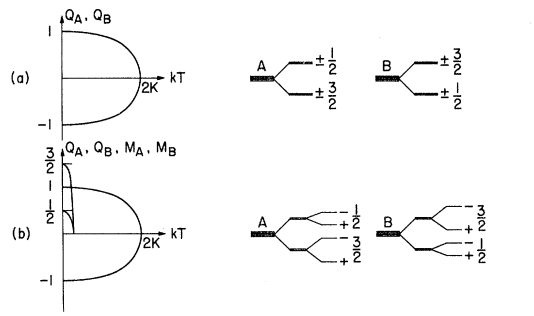

FIG. 6. (a) Pure antiquadrupolar ordering ($J = 0$, $K < 0$) and (b) well-separated ferrimagnetic and antiquadrupolar transitions ($|K| \gg J > 0$).

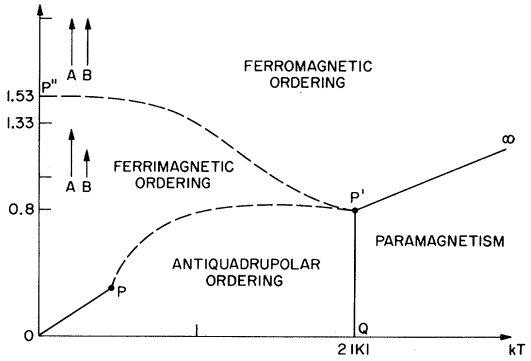

FIG. 7. Phase diagram for $h=0$, $K<0$, $J>0$. Dashed lines indicate first-order transitions.

and indeed the entropy variation associated with each transition is $\Delta S \simeq R\ln 2$.[8] The spin Hamiltonian responsible for the cooperative transitions may consequently be represented at least qualitatively by our model Hamiltonian (1) with $J<0$ and $K>0$. (The latter follows because between the two transitions, all Dy^{3+} ions are equivalent). Because of the observed quasidegeneracy, we may neglect any crystalline field. J is an ordinary superexchange interaction, and K is either a magnetostrictive or indirect quadrupole-quadrupole interaction, as discussed in the Introduction.

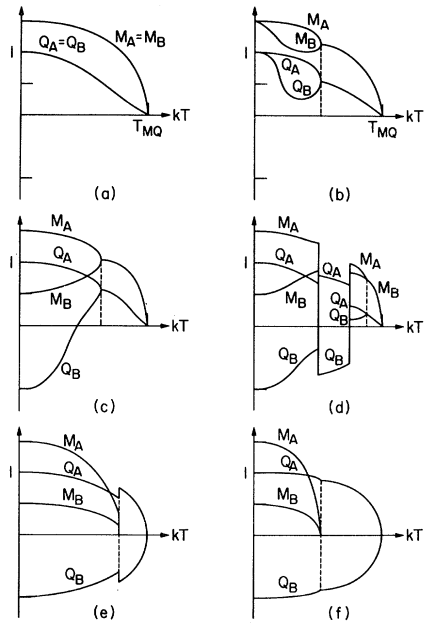

FIG. 8. Thermal variation of M_A, M_B, Q_A, and Q_B: (a) a single second-order transition; (b) and (c) two second-order transitions; (d) $0.81>J>0.80$ four transitions, an intermediate antiquadrupolar ordering; (e) a second-order antiquadrupolar transition and a first-order dipolar transition; and (f) two second-order transitions.

Since the two phase transitions are well separated (3 and 14 °K), we must have $J \ll K$ as in our phase diagram. In particular, the crystal distortion is unaffected by the magnetic transition, i.e., $Q \simeq 1$ at the magnetic transition (as we have seen, the sign of J, which here must be negative, has no bearing on the phase diagram in the J, T plane).

The magnetic character of the transition at 14 °K is shown by the influence of a magnetic field h_x or h_y which induces the crystallographic distortion (tetragonal to orthorhombic) well above 14 °K[18]; the splitting of the quadruplet explains the Ising character of the magnetic transition (spin flip), although the orthorhombic distortion is very weak. To the two possible signs of Q between 3 and 14 °K correspond two domains; when h is applied, the sign of Q is determined, i.e., one type of domain is selected. Finally, the values of the different g factors are different in $DyVO_4$ and in our model, since we neglect all the excited states and the possible Heisenberg character of the interactions as well as more complex types of exchange. For the same reason, it is difficult to get a correct value

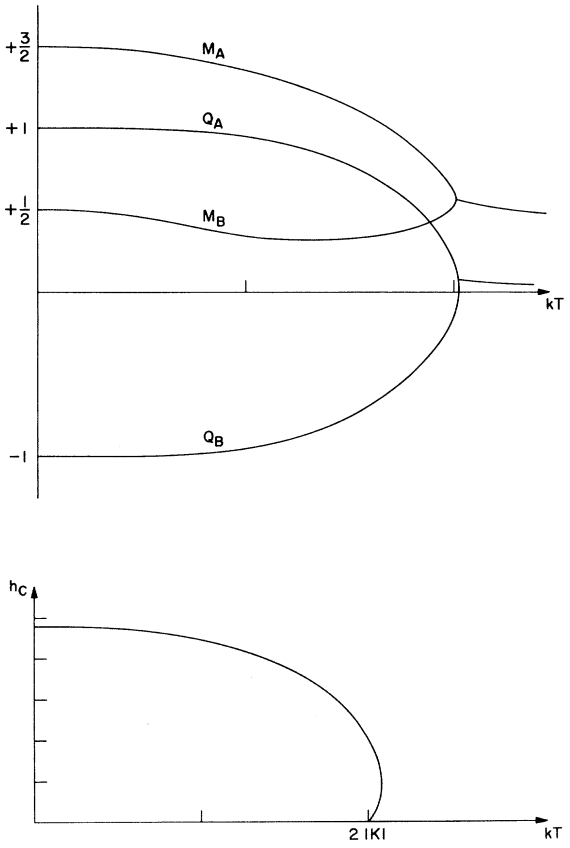

FIG. 9. Influence of h on antiquadrupolar transition (a) variation of M_A, M_B, Q_A, and Q_B for $J=0$, $Sh=1.0$ and (b) thermal variation of the critical field h_c.

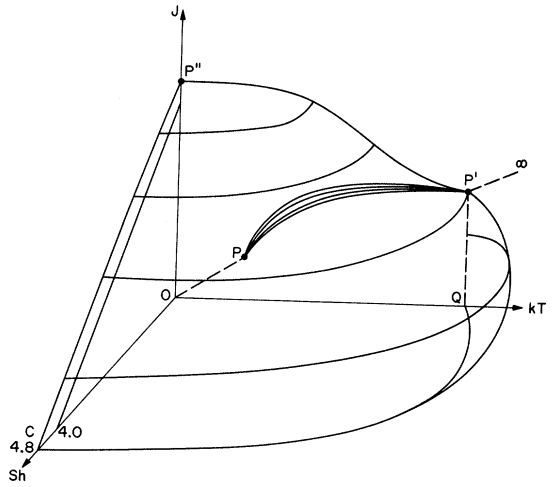

FIG. 10. Influence of h on the phase diagram ($K<0$).

of the parameters J and K of the true spin Hamiltonian, since we are dealing with an *effective* spin $\frac{3}{2}$.

With a change of interpretation, the Ising model can be made to correspond somewhat more closely to the situation in $DyVO_4$. We assume that there is no relation between the quantization axis of the Ising system and the z axis of the crystal. A $|\pm\frac{3}{2}\rangle$ state ($Q=+1$) represents a quadrupole elongated along the x axis and a $|\pm\frac{1}{2}\rangle$ state ($Q=-1$) a quadrupole flattened along x or a quadrupole elongated along y. This choice is more adapted to the description of $DyVO_4$ because of the two possible domains which appear below T_Q. The introduction of dipolar interactions selects the domain with $Q=+1$ preferentially.

The possibility of two successive second-order phase transitions is confirmed by symmetry considerations.[19] The high-temperature group is $G=I(4_1/a)md$. Since the transition leaves the unit cell unchanged, we may consider only the point group $G_0=(4/m)mm$. Now, following Landau and Lifschitz, we may classify the coordinates of the quadrupoles of the two Dy^{3+} ions in the unit cell according to the representations of G. We find that a "ferromagnetic" arrangement of quadrupoles transforms according to the B_{1g} representation, whose kernel is $Imma$. Consequently, such an ordering leads to an orthorhombic symmetry, and it may be second order since B_{1g} is a real one-dimensional representation. Then the dipolar ordering corresponds to a real one-dimensional representation of the group $Imma$ with $k=0$; it is described by a magnetic group isomorphic to $Imma$.

VII. CONCLUSIONS

Our model Hamiltonian (1) may describe qualitatively some systems where two-order parameters may be defined: crystals with crystallographic and magnetic ordering, for instance. We have shown that it describes qualitatively the magnetic properties of $DyVO_4$. It would be interesting to compare our results with the results for a similar Heisenberg Hamiltonian where new elementary excitations appear which may be called magnetic librons. Even the simple model considered here shows the great complexity which is possible when two or more kinematically coupled order parameters contribute to the internal energy. We have found first- and second-order phase transitions to states of quadrupolar and antiquadrupolar order; ferro-, antiferro-, and ferrimagnetism, and two combinations of these. The critical indices of the quadrupolar order depend, even in the mean-field approximation, on the nature of the interactions.

It should also be mentioned that quadrupolar order can be detected experimentally by x-ray diffraction, even if the lattice remains undistorted. This is because the anisotropic part of the x-ray form factor is altered by the alignment of the electronic quadrupoles.

Quantitative calculation for specific substances requires a more detailed knowledge of the exchange parameters and of the form of the exchange interaction than we have at present. The Ising system treated here illustrates, however, the qualitatively new effects which are to be anticipated.

*Work performed under the auspices of the U. S. Atomic Energy Commission.

†Guest scientist, on leave from Centre d'Etudes Nucléaires, Grenoble, France.

[1]T. J. Krieger and H. M. James, J. Chem. Phys. 22, 796 (1954).

[2]M. Blume and Y. Y. Hsieh, J. Appl. Phys. 40, 1249 (1969).

[3]H. W. Capel, Physica 32, 966 (1966).

[4]R. B. Griffiths, Physica 33, 689 (1967).

[5]R. E. Watson and M. Blume, Intern. J. Quant. Chem. Suppl. 1, 645 (1967).

[6]F. Rys, Helv. Phys. Acta 42, 606 (1969).

[7]M. Blume, V. J. Emery, and R. B. Griffiths, Phys. Rev. A 4, 1071 (1971).

[8]A. H. Cooke, D. M. Martin, and M. R. Wells, Solid State Commun. 9, 519 (1971).

[9]A. H. Cooke, D. M. Martin, and M. R. Wells, J. Phys. (Paris) C1, 488 (1971).

[10]F. Sayetat, J. X. Boucherle, M. Belakhovsky, A. Kallel, F. Tcheou, and H. Fuess, Phys. Letters 35A, 361 (1971).

[11]R. J. Elliott and M. F. Thorpe, J. Appl. Phys. 39, 802 (1968).

[12]P. M. Levy, Phys. Rev. 135, A155 (1964).

[13]See H. Falk, Am. J. Phys. 38, 858 (1970).

[14]L. D. Landau and E. M. Lifschitz, *Statistical Physics*, 2nd ed. (Addison-Wesley, Reading, Mass., 1969), p. 424.

[15]C. P. Bean and D. S. Rodbell, Phys. Rev. 126, 104 (1962).
[16]R. B. Griffiths, Phys. Rev. Letters 24, 715 (1970).
[17]G. Will and W. Schäffer, J. Phys. C 4, 811 (1971).
[18]C. J. Ellis, K. A. Gehring, M. J. M. Leask, and R. L. White, J. Phys. (Paris) 1, 1024 (1971).
[19]J. Sivardière, Phys. Rev. B (to be published).

PHYSICAL REVIEW B VOLUME 5, NUMBER 3 1 FEBRUARY 1972

Magnetic Susceptibility and Low-Temperature Specific Heat of Dilute Transition-Metal Alloys*

Helmut Claus†
Department of Metallurgy, University of Illinois at Champaign-Urbana, Illinois 61801
(Received 18 June 1971)

Magnetic-susceptibility measurements between 4 and 800 °K and specific-heat measurements between 1.5 and 4.2 °K are reported for a series of dilute *Rh*-Mn, *Mo*-Fe, *Mo*-Co, and *Au*-Fe alloys in the concentration range 0.02–0.7 at.%. The solute susceptibility $\Delta\chi$ of all alloys shows local-moment behavior and scales with the concentration over a wide concentration range, but large deviations from simple Curie-Weiss behavior, qualitatively the same for all alloys, are observed. This deviation consists of a rapid increase of $\Delta\chi$ at low temperatures. A pronounced field dependence of $\Delta\chi$ and large specific-heat anomalies at these temperatures strongly suggest that this rapid increase in $\Delta\chi$ arises from solute-solute interactions. This anomalous part of $\Delta\chi$ can readily be separated from the part due to isolated solute atoms. The conclusion is drawn that scaling of the solute susceptibility with concentration does *not* necessarily signify that the alloys are "dilute" in the conventional sense.

I. INTRODUCTION

In recent publications[1,2] we reported that dilute alloys of Mn in Rh exhibit a local moment but that the magnetic susceptibility does not show simple Curie-Weiss behavior. It was found that the solute susceptibility contains a very substantial temperature-independent term and at low temperatures increases much faster than predicted by the Curie-Weiss equation. Since these deviations from Curie-Weiss behavior scale with the Mn concentration, they were attributed to single-impurity effects. Large temperature-independent terms in the solute magnetic susceptibility of alloys exhibiting local moments have also been reported for dilute alloys of Mn in Mo,[2] Co in Mo,[3] and V in Au.[4] As in the *Rh*-Mn alloys, the magnetic susceptibility of *Rh*-Fe alloys increases at low temperatures much faster than a simple Curie-Weiss equation would predict.[5,6] Generally, deviations from Curie-Weiss behavior of the magnetic susceptibility are observed for almost all dilute alloys exhibiting local moments.[7–9] This is not surprising since the Curie-Weiss equation can only be considered as a convenient interpolation formula between a high-temperature Curie law and a finite zero-temperature solute susceptibility as predicted by both Kondo-type and fluctuation theories for the single-impurity limit.[9–11] In the absence of general theoretical predictions for the detailed temperature dependence of the magnetic susceptibility for dilute magnetic alloys, the observed systematic deviation from Curie-Weiss behavior should give valuable information about the electronic structure of a single magnetic impurity.

Quite recently, it has been demonstrated that even in very dilute alloys, interactions between solute atoms can contribute significantly to the magnetic susceptibility.[12,13] The question then arises as to whether the deviations from Curie-Weiss behavior observed earlier do indeed reflect properties of noninteracting impurity states. To investigate this question, we have made a magnetic study of a variety of dilute alloy systems over a wide temperature range. In addition, low-temperature specific-heat measurements were performed on the same alloys.

II. EXPERIMENTAL DETAILS

A. Alloy preparation

The following new alloys were prepared: Mo with 0.02-, 0.1-, 0.2-, 0.5-, and 0.7-at.% Fe, Mo with 0.1- and 0.4-at.% Co, Rh with 0.1- and 0.6-at.% Mn, and Au with 0.02- and 0.1-at.% Fe. The solvent materials Mo, Rh, and Au were 99.999% pure as quoted by the supplier. The solute materials were 99.99% pure. Before alloying, the magnetic susceptibility and the low-temperature specific heat of the solvent materials were determined. No significant amounts of magnetic impurities could be detected. For each of the four alloy systems investigated, a master alloy with about 3-at.% solute